MAPPING OF SEA BOTTOM TOPOGRAPHY IN SHALLOW SEAS BY USING A NAUTICAL RADAR

Hessner K.[1] , K. Reichert[1], and W. Rosenthal[2]
[1]Ocean SensWare -, GKSS Technologie Zentrum, Max-Planck-Str., Geesthacht, D- 21502, Germany, hessner@gkss.de
[2]GKSS , Geesthacht, D-21502 Germany, rosenthal@gkss.de

KEYWORDS: Nautical Radar, Wave Monitoring, Dispersions Relation, Bottom Topography

ABSTRACT

A new method to obtain underwater bottom topography in shallow waters based on the analysis of nautical radar images is presented. In shallow waters local variations in the bottom topography yield to a modulation of long surface waves by different processes like refraction shoaling, defraction. As ocean surface waves are visible in nautical radar images, local wave refraction can be observed in such radar images. The wave monitoring system WaMoS II based on a nautical radar has proven to be a powerful tool to monitor ocean waves in time and space. By analysing a sequence of nautical radar images by a temporal Fourier transform it is possible to derive local wave information. The local water depth can be inferred from this wave information by applying the linear wave theory. In order to estimate the capability of the proposed method, simulations are performed for different wave characteristics and water depths. The method has been verified with WaMoS II radar data, captured south west off Heligoland island located in the German Bight. The analysis of the radar data shows significant modulation of ocean waves near the shore. The local water depths inferred from the radar images are in good agreement with traditionally obtained water depths from sea charts. These promising results suggests the possibility of using WaMoS II to monitor operationally morphodynamics in coastal zones.

1 INTRODUCTION

The detailed knowledge of the bottom topography in shallow waters is crucial for off-shore activities such as shipping, fishery, harbour constructions and routing of oil pipes as well as for morhpodynamic investigations. Water depth information is traditionally obtained by ship based echo sounders. Despite that these surveys are rather expensive and time consuming they can not be used in very shallow sea areas not reachable for ships. Especially for these regions considerable interest has been shown recently in the use of remote sensing techniques to determine the water depth.

It is known that in shallow seas the local bottom topography has a significant influence on the propagation of the surface waves. More general, as waves move into shallow water (water depth less than half of the wave length) their periods (frequencies) remain constant but their propagation speeds and hence their wave lengths decrease (wave numbers increase). With the knowledge of the wave period and corresponding local wave length the local water depth can be determined by using the dispersion relation of linear surface waves. Early activities to remotely obtain water depth information based on this effect were carried out in the 1940s, where the local water depth was estimated from wave patterns from aerial photographs for military purposes (Hart et al, 1945).

An other method to remotely acquire water depth information is based on the analysis of the modulation of the radar backscatter in synthetic aperture radar (SAR) images. Based on an imaging mechanism for under water bottom topography (Alpers and Hennings, 1984), inverse techniques to estimate the local water depth from SAR images have been developed (Vogelzang et al, 1995, Greidanus, 1997). These techniques can only be applied in shallow seas with high current speed (~ 1m/s) and requires a certain geometry between, bathymetry gradient, current and radar look direction. In order to determine the position of breaker bars in the surf zone, Holman et al, 1991 described a method based on the localisation of breaking waves in video images.

One technique to remotely measure ocean waves is WaMoS[1] II. This system is based on a conventional nautical X-band radar generally used for traffic control and navigation purposes. By analysing the spatial and temporal evolution of radar backscatter signals from the sea surface this system allows to obtain unambiguous direction wave information (Young et al, 1985, Ziemer, 1991, Ziemer and Günther, 1994, Nieto et al, 1998). A first attempt to infer also water depth information with this system was carried out by Outzen (1998). Assuming a flat bottom within the analysis area, the mean water depth can be determined from the position of the wave energy located in the measured 3d image spectrum.

First steps to infer spatially varying water depth from nautical radar images have been carried out by Paul Bell (1998). By analysing the coherence of wave patterns between successive nautical radar images, the local wave velocity is estimated. Together with the corresponding wave frequency from a wave rider buoy, the local water depth can be determined by using the dispersions relation for linear gravity waves.

Here a similar method based on the determination of the wave frequency and corresponding wave number both from nautical radar images is described. The paper is organised as following: In section 2 the theory of the method is presented. In section 3 simulations are performed in order to test the proposed method and in section 4 results of radar measurements taken on Heligoland are presented and compared with traditionally obtained bathymetry data. In section 5 summary and conclusions are given.

[1] **Wa**ve **Mo**nitoring **S**ystem

2 THEORY

In the absence of a surface current, the relationship between the radian wave number k (= $2\pi/l$) and frequency w (=$2\pi/t$) for linear gravity waves is given by the dispersion relation:

$$w^2 = gk\tan(kd)\,, \tag{1}$$

where g is the acceleration of gravity, d the water depth, l the wave length, and t the wave period. Rearranging of (1) yields to:

$$d(w,k) = \frac{1}{k}\operatorname{arctanh}\left(\frac{w^2}{gk}\right). \tag{2}$$

so that the water depth d becomes a function of wave frequency ω and the corresponding local wave number k. Figure 1 shows water depth d as function of ω and k (P and λ, respectively).

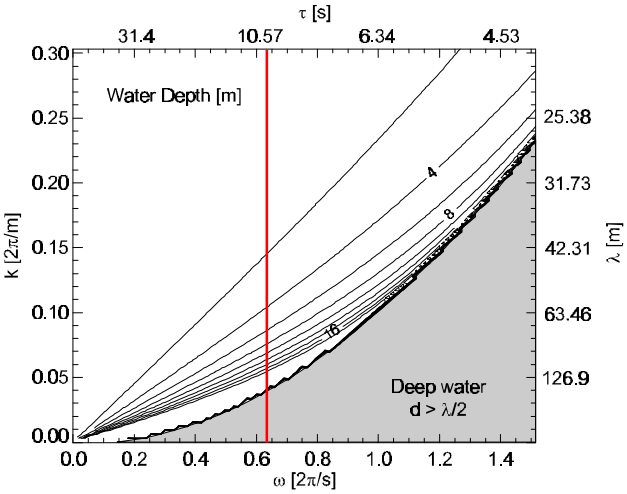

Fig. 1: Contour plot of the water depth d as function of the angular wave number k (wave length λ= 2π/k) and wave frequency w (wave period P= 2π/w). The contours give the water depth in meter with 2m intervals. The red line marks the frequency for which a k-tansect is shown in Fig 2.

Measurements have shown, that the wave frequency w does not change significantly as waves propagate from deep (d > 0.5 l) into shallower water. Fig. 1 shows that k increases (l decreases) as a wave with a certain frequency w propagate into shallower areas. The grey area marks the area in the w-k space where the water depth is too large (deep water condition: d > l/2), to influence the waves characteristics so that the wave number is independent of the water depth.

The accuracy in determining the water depth by using Eq. 2 depend strongly on the d/λ ratio. If d/λ exceeds 0.5 the local water depth d has no measurable effect on the wave number. In addition if the ratio d/λ is very small (< 1/20, shallow water) also small changes of d lead to large changes in k. Figure 2a shows the water depth d as a function of the wave number k for a wave with a frequency of w = 0.628 rad/s (t = 10 s).

The figures demonstrate the sensitivity of water depth determination on the accuracy of the observed wave number k. Thus waves of considerable small w and k (large t and l, respectively) are required in order to obtain reliable water depth information.

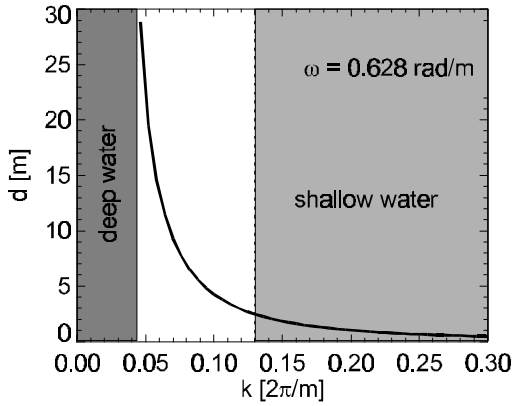

Fig. 2: Water depth d as function of the angular wave number k for a wave frequency of w = 0.628 rad/s (t = 10s).

Therefor the observation of ocean waves with periods of more than 8 s is most suitable for the proposed method.

2.1 Determination of the Local Wave Number

Assuming that the sea surface elevation z is represented as a linear superposition of monochromatic waves characterised by their wave vector $\boldsymbol{k}$ = (k_x,k_y) , amplitude z_0, and angular frequency w, it can be expressed by:

$$z(\boldsymbol{r},t) = \sum_{\boldsymbol{k},w}\left(z_0(\boldsymbol{k},w)\exp(i(\boldsymbol{kr}-wt)+c.c.\right). \tag{3}$$

where $\boldsymbol{r}$ = (x,y) is the position in space, t the time, and c.c. the complex conjugate. In this case the complex sea surface elevation can also be expressed as Fourier series in time:

$$\begin{aligned} z(\boldsymbol{r},w_n) &= FFT\left[z(\boldsymbol{r},t)\right] \\ &= \sum_{j=0}^{N-1}\left(z(\boldsymbol{r},t_j)\exp(-i(-w_n t_j)\right)Dt\,, \end{aligned} \tag{4}$$

where w_n are the discrete frequency values

$$w_n \equiv \frac{n}{N\Delta t}, \qquad n = -\frac{N}{2},\ldots,\frac{N}{2}\,, \tag{5}$$

Δt the temporal resolution (sampling rate), and N the number of samples.

For a monochromatic wave with a frequency w_n the complex surface elevation is given by:

$$\begin{aligned} z(\boldsymbol{r},w_n) &= z_0(\boldsymbol{k},w_n)\exp(i(\boldsymbol{kr})NDt \\ &= \mathrm{Re}\left[z(\boldsymbol{r},w_n)\right] + i\,\mathrm{Im}\left[z(\boldsymbol{r},w_n)\right]. \end{aligned} \tag{6}$$

The amplitude z_0 and phase F of the wave is given by:

$$z_0(\boldsymbol{k},\boldsymbol{r},w_n) = \sqrt{\mathrm{Re}\left[z_0(\boldsymbol{r},w_n)\right]^2 + \mathrm{Im}\left[z_0(\boldsymbol{r},w_n)\right]^2}\,. \tag{7}$$

$$F(\boldsymbol{k},\boldsymbol{r},w_n) = \boldsymbol{kr} - wt = \arctan\left(\frac{\mathrm{Im}[z_0(\boldsymbol{r},w_n)]}{\mathrm{Re}[z_0(\boldsymbol{r},w_n)]}\right). \quad (8)$$

Assuming that the variation of the local wave number is small ($\partial\boldsymbol{k}/\partial\boldsymbol{r} \approx 0$), $\boldsymbol{k}(\boldsymbol{r},w_n)$ can be computed by:

$$\boldsymbol{k}(\boldsymbol{r},w_n) = \frac{\P F(\boldsymbol{k},\boldsymbol{r},w_n)}{\P \boldsymbol{r}}. \quad (9)$$

3 SIMULATIONS

In order to estimate the capability of the method, simulations of monochromatic wave image sequences are performed. The images are stored in a pixel matrix which corresponds to a integration domain W_r given by:

$$W_{\boldsymbol{r},t} \equiv [0,X]\times[0,Y]\times[0,T]. \quad (10)$$

where X and Y are the spatial extension of each wave image and T is the length of the image sequence. Corresponding to the radar measurement presented later (Section 4.2), the extension and resolution of the integration domain is defined as $X = 128\Delta x$, $Y = 64\Delta y$ with the spatial resolution of $\Delta x = \Delta y = 4.9$m. The image sequence consists of 64 single images so that $T = 64\Delta t$. The temporal resolution is $\Delta t = 1.89$ s which coincides with the radar rotation time. These values yield to a resolution in frequency of $\Delta w = 2\pi/T = 0.052$ rad/s and a critical Nyquist limit of $w_c = p/\Delta t = 1.66$ rad/s.

For a wave with w_n and a given water depth $d(\boldsymbol{r})$ the corresponding local wave number $\boldsymbol{k}(\boldsymbol{r})$ can be determined by using the dispersion relation (Eq. 1). Since the rotation of $\boldsymbol{k}$ vanishes ($\nabla\times\boldsymbol{k} \approx 0$) the local phase of the wave can be reconstructed by:

$$F(\boldsymbol{k},\boldsymbol{r},w_n) = F(\boldsymbol{k},\boldsymbol{r},w_n,\boldsymbol{r}_0) = \int_{\boldsymbol{r}_0}^{\boldsymbol{r}} \boldsymbol{k}(\boldsymbol{s})d\boldsymbol{s} - w_n t. \quad (11)$$

The corresponding surface elevation $z(\mathbf{r},t)$ is given by Eq. 6.

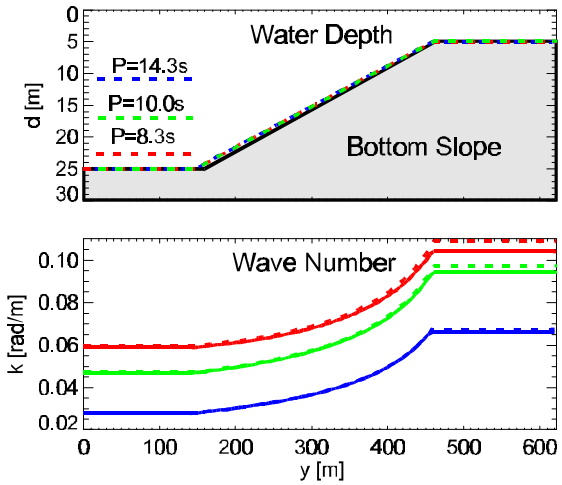

Fig. 3: Transect of the water depth d (upper panel) and corresponding wave number k (lower panel). The solid line corresponds to the prescribed start d and k the dotted lines to the analysis results. The colour indicate the different wave frequencies for which the simulations were carried out.

Figure 3 shows a transect of water depth d (left panel) and wave number k (middle panel) along the y-axis of the integration domain. The solid lines represent the prescribed d and corresponding k and F, the dotted lines indicated the analysis results and the colours indicate the different wave frequencies for which the simulation where carried out.

The figure shows an increasing wave number as the water depth decreases. The wave number obtained by the analysis of the simulated surface elevation shows a good agreement with the simulated one. Especially the water depth is well reproduced. These results demonstrate the capability of the proposed method.

4 MEASUREMENTS

4.1 WaMos II set up on Heligoland

The radar data presented in this section were obtained from the WaMoS II site located on Heligoland in the German Bight. The radar antenna of the WaMoS II has been installed about 80 m above the sea level.

Figure 6 shows a WaMoS II radar image obtained on Okt, 25, 1998, 21:00 UTC. At that time the wind was blowing from West with a speed of about 22 m/s.

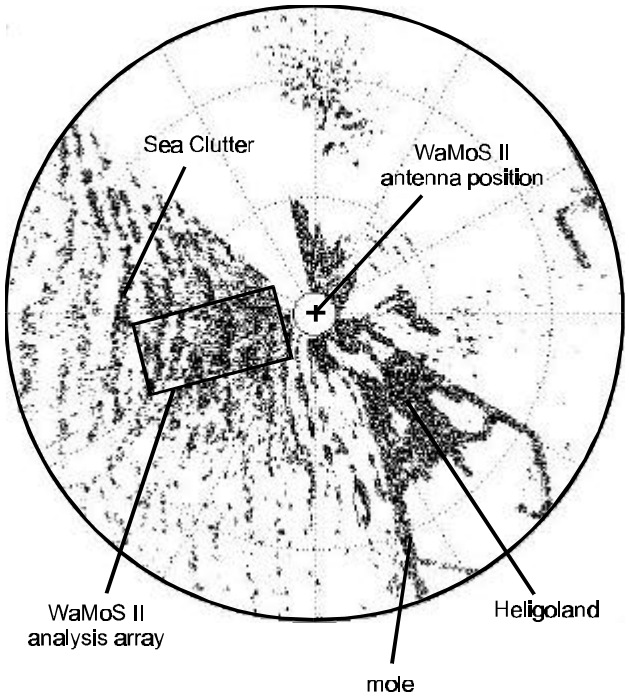

Fig. 4: WaMoS II polar radar image obtained on Oct. 25, 1998, 21:00 UTC from the WaMoS II Station Heligoland. The WaMoS II radar antenna (+) is located in the centre of the image. South-east of the antenna the island with the mole is visible as dark patches. West and south-west of the antenna radar signatures in form of wave pattern are visible. The box indicates the WaMoS II analysis area.

Aside from signatures of the island Heligoland, the radar image displays surface wave signatures in form of wave crest patterns aligned almost north-southward. The standard

WaMoS II analysis yields in the southern part a significant wave height of about 4 m with a peak wave period of 12 s and a peak wave direction of 271 degree.

Ocean waves become visible in nautical radar due to the modulation of the radar backscatter (ds_0) by the long ocean waves (Alpers and Hasselmann, 1982, Wenzel, 1990). Thus the grey level of the radar images depend on the height of the observed waves. Especially the space-time behaviour of the sea surface elevation is reproduced by the grey level variations. For the proposed method we assume that the sea surface elevation due the long waves is linear related to ds_0 and hence to the grey level in the radar image. In this case the surface elevation $\zeta(\boldsymbol{r},t)$ in Eq. 4 can be replaced by grey scale of the radar images and $\boldsymbol{k}(\boldsymbol{r})$ can be determined directly from the radar images.

4.2 Results

The analysis is carried out within the area of 1200m × 600m located south-westward of the WaMoS II antenna (see Fig. 4). For each measurement 64 single images were taken.

As an example the results for the peak wave with t = 12 s are shown in Figures 5-7.

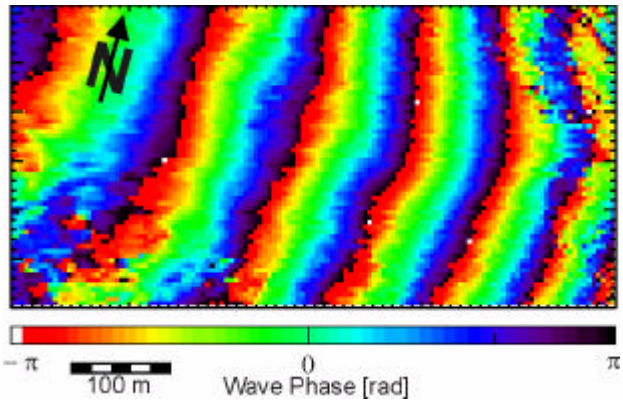

Fig. 5: Phase F of the 12 s wave as obtained by WaMoS on Oct. 25, 1998. The North arrow indicate the orientation of the image. The colour coding corresponds to the phase of the wave.

Figure 5 shows clearly the spatial coherence of the wave phase. The eastward propagating wave is clearly visible as striped pattern aligned perpendicular to the wave propagation direction. This shows that the assumption of the local validity of the dispersion relation permits the extraction of water depth from radar image sequences. Only in the upper right and lower left corner of the image incoherent pattern due to weak radar signals are visible. Due to the interaction of the wave with the bottom topography the wave length decreases from about 150m (upper left corner) to 80m (lower right corner). Furthermore, in the upper left corner a slight anticlockwise veering of the wave towards the coast is visible. This contraction of the wave can also be seen in the wave number image (Fig. 6).

As the wave propagates from the deeper water (upper left part) towards the coast (right part of the Fig. 6) the wave number increases. In the small wave numbers in the lower left part of Fig.6 are supposed to be invalid, as the phase image show irregularities in this part.

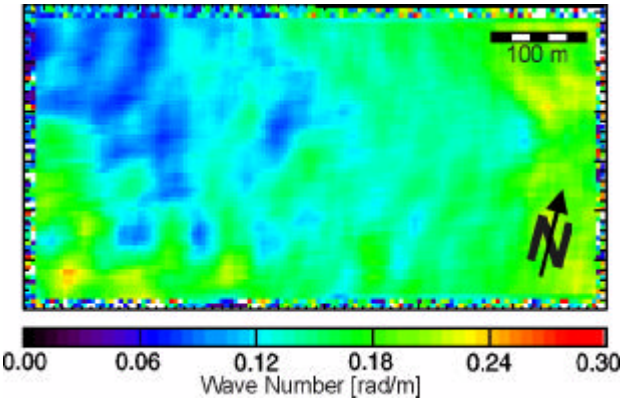

Fig. 6: Wave number k of the 12 s wave.

Figure 7 shows the corresponding water depth for this area. The colour coding corresponds to the water depth inferred from the radar measurement, the isolines are from the sea chart. Note that for the display of the wave number and the water depth has been averaged over a 3×3 pixel area.

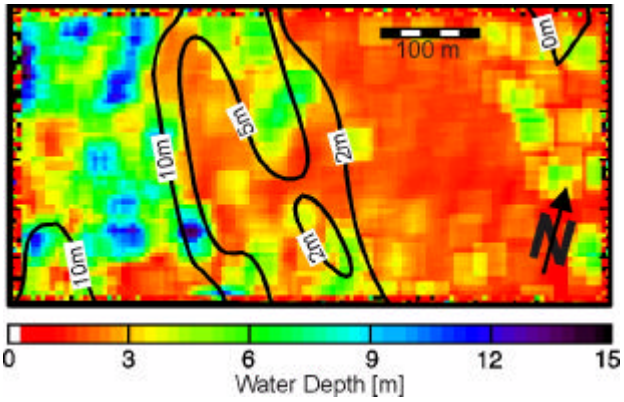

Fig. 7: Bottom topography in the analysis area: The colour coding corresponds to the water depth inferred from the 12 s wave phase, the isolines give the waver depth from the sea chart (No. 88 BSH)

The comparison of the water depth inferred from the radar images and from the sea chart are in good agreement. The absolute values as well as the local variation are reproduced. The absolute deviation of the water depth inferred by WaMoS and the sea chart can be explained by the unknown absolute water level at the time of measurement. The water depth within the sea charts are relative to minimum low water at spring time. Nevertheless the general features of the bottom topography are well reproduced.

In general such depth information can be obtained for any w_n frequency. Averaging of the different depth information would enhance the reliability of the obtained depth information.

5 CONCLUSIONS

A method to derive local water depth in shallow water from nautical radar images is presented. It has be shown that by using the dispersion relation for linear surface waves it is possible to obtain spatial varying water depth information. The general capability of the proposed method has been proven by

simulations. The practical capability has been demonstrated by analysing radar images captured by WaMoS II south-west off Heligoland island. The radar images show significant modulation of the ocean waves as they propagate towards the coast. The absolute values as well as the spatial variations of the obtained local water depth from WaMoS II measurements show a good agreement with the water depth from the sea chart.
These promising results demonstrate the capability to use WaMoS to monitor the bathymetry in shallow waters.

ACKNOWLEDGEMENTS

The Heligoland project is supported by the Bundesanstalt für Wasserbau, Germany (BAW), and the GKSS research centre and the Technologie Transferzentrale Schleswig-Holstein.

REFERENCES

Alpers, W., and K. Hasselmann, 1982. Spectral Signal to Clutter and Thermal Noise Properties of Ocean Wave Imaging Synthetic Aperture Radars. Int. J. Rem. Sens., 3, pp. 423-446.

Alpers, W., and I. Hennings, 1984. A theory for the imaging mechanism of under water boootm topography by real and synthetic aperture radar. J.Geophys.Res., 89, pp. 10 529-10 546.

Bell, P., 1998. Bathymetry derived from an analysis of X-Band marine radar images of waves. Proceedings fo the Oceanology International 98, pp. 535-543.

Greidanus, H., 1997. The use of radar for bathymetry in shallow seas. The Hydrographic Journal, 83, pp. 13-18.

Hart, C.A., and E.A. Miskin, 1945. Developments in the method of determination of beach gradients by wave velocity. Air survey research paper No. 15, pp. 1-54.

Holman R.A., T.C. Lippmann, P.V.O'Neill, and K. Hathaway, 1991. Videao estimation of subaerial beach profiles. Marine Geology, 97, pp. 225-231.

Nieto, J.C., K. Reichert, J. Dittmer, and W., Rosenthal, 1998. WaMoS II: A wave and current monitoring system. Proceed. Of the COST 714 conference on directional wave spectra, Paris.

Outzen, O., 1998. Bestimmung der Wassertiefe und der oberflächennahen Strömung mit einem nautischen Radar. Diplomarbeit Fachbereich Geowissenschaften Universität Hamburg, GKSS-Forschungszentrum, Geesthacht, pp. 90.

Vogelzang, J., H. Greidanus, G.J. Wensink, and R. van Swol, 1995. Mapping of sea bottom topography with ERS-1 C-Band SAR. BCRS report 94-27, Rijkswaterstaat, The Netherlands pp. 108.

Wetzel, L.B., 1990. Electromagnetic Scattering from the Sea at Low Grazing Angles. Surface Waves and Fluxes, Kluwer Academic Publishers, Netherlands , Vol. II, pp. 41-108

Young, I.R., Rosenthal W. and Ziemer F., 1985. A Three-dimensional analysis of marine radar images for the determination of ocean wave directionality and surface currents. J.Geophys.Res., 90, pp. 1049 - 1059.

Ziemer, F., 1991. Directional Spectra from Shipboard Navigation Radar during LEWEX. Directional Ocean Wave Spectra, The John Hopkins University, pp. 80-84.

Ziemer, F. and Günther, H., 1994. A system to monitor ocean wave fields. Proc. 2Nd. Int. Conf. On Air-Sea Interaction and Meteorology and Oceanography of the Coastal Zone. Lisboa, September 22-27, 1994.